

Bi-allelic variants in the ER quality-control mannosidase gene *EDEM3* cause a congenital disorder of glycosylation

Daniel L. Polla,^{1,2,22} Andrew C. Edmondson,^{3,22} Sandrine Duvet,⁴ Michael E. March,⁵ Ana Berta Sousa,^{6,7} Anna Lehman,⁸ CAUSES Study, Dmitriy Niyazov,⁹ Fleur van Dijk,¹⁰ Serwet Demirdas,¹¹ Marjon A. van Slegtenhorst,¹¹ Anneke J.A. Kievit,¹¹ Celine Schulz,⁴ Linlea Armstrong,⁸ Xin Bi,¹² Daniel J. Rader,^{5,12,13} Kosuke Izumi,³ Elaine H. Zackai,³ Elisa de Franco,¹⁴ Paula Jorge,^{15,16} Sophie C. Huffels,¹ Marina Hommersom,¹ Sian Ellard,^{14,17} Dirk J. Lefeber,^{18,19} Avni Santani,^{20,21} Nicholas J. Hand,^{13,22} Hans van Bokhoven,^{1,22} Miao He,^{21,22,*} and Arjan P.M. de Brouwer^{1,22,*}

Summary

EDEM3 encodes a protein that converts Man₈GlcNAc₂ isomer B to Man_{7,5}GlcNAc₂. It is involved in the endoplasmic reticulum-associated degradation pathway, responsible for the recognition of misfolded proteins that will be targeted and translocated to the cytosol and degraded by the proteasome. In this study, through a combination of exome sequencing and gene matching, we have identified seven independent families with 11 individuals with bi-allelic protein-truncating variants and one individual with a compound heterozygous missense variant in *EDEM3*. The affected individuals present with an inherited congenital disorder of glycosylation (CDG) consisting of neurodevelopmental delay and variable facial dysmorphisms. Experiments in human fibroblast cell lines, human plasma, and mouse plasma and brain tissue demonstrated decreased trimming of Man₈GlcNAc₂ isomer B to Man₇GlcNAc₂, consistent with loss of *EDEM3* enzymatic activity. In human cells, Man₅GlcNAc₂ to Man₄GlcNAc₂ conversion is also diminished with an increase of Glc₁Man₅GlcNAc₂. Furthermore, analysis of the unfolded protein response showed a reduced increase in *EIF2AK3* (*PERK*) expression upon stimulation with tunicamycin as compared to controls, suggesting an impaired unfolded protein response. The aberrant plasma N-glycan profile provides a quick, clinically available test for validating variants of uncertain significance that may be identified by molecular genetic testing. We propose to call this deficiency *EDEM3*-CDG.

The endoplasmic reticulum-associated degradation (ERAD) pathway recognizes misfolded proteins that will be targeted and translocated to the cytosol and degraded by the proteasome.^{1–4} The best characterized system is dedicated to N-linked glycoproteins: the glycoprotein ERAD (gpERAD) pathway. Proteins that fail to fold or assemble properly are subjected to degradation via specific trimming of high-mannose-type glycans in the lumen of the ER.^{5,6} In mammals, *EDEM2* and *ERmanI* are known to primarily catalyze the first step, conversion of Man₉GlcNAc₂ (M9) to Man₈GlcNAc₂ isomer B (M8B).^{7–9} *EDEM3* and *EDEM1*

are further involved in catalyzing the second step, the conversion of M8B to Man₇GlcNAc₂ (M7).^{7–12} These products are then recognized by lectin OS-9 in the ER lumen and targeted for degradation in the cytosol.¹³

Cells can degrade misfolded proteins from the secretory pathway by using the glycan-dependent and glycan-independent ERAD pathways.^{14–16} The presence of misfolded ER proteins is harmful to cells and is involved in several congenital disorders of glycosylation (CDGs),^{17–20} such as PMM2-CDG (MIM: 212065), MPI-CDG (MIM: 602579), ALG6-CDG (MIM: 603147), DPM1-CDG (MIM: 608799),

¹Department of Human Genetics, Donders Institute for Brain, Cognition, and Behavior, Radboud University Medical Center, 6500 HB Nijmegen, the Netherlands; ²CAPE Foundation, Ministry of Education of Brazil, Brasília, Brazil; ³Department of Pediatrics, Division of Human Genetics, Children's Hospital of Philadelphia, Philadelphia, PA 19104, USA; ⁴Université de Lille, CNRS, UMR 8576 – UGSF – Unité de Glycobiologie Structurale et Fonctionnelle, F-59000 Lille, France; ⁵Center for Applied Genomics, Children's Hospital of Philadelphia, Philadelphia, PA 19104, USA; ⁶Serviço de Genética Médica, Hospital de Santa Maria, Centro Hospitalar Universitário Lisboa Norte, 649-035 Lisboa, Portugal; ⁷Faculdade de Medicina da Universidade de Lisboa, 1649-028 Lisboa, Portugal; ⁸Department of Medical Genetics, University of British Columbia, Vancouver, BC V6H 3N1, Canada; ⁹Tulane School of Medicine, University of Queensland, 1315 Jefferson Highway, New Orleans, LA 70121, USA; ¹⁰North West Thames Regional Genetics Service, London North West University Healthcare NHS Trust, Watford Road, Harrow, HA1 3UJ London, UK; ¹¹Department of Clinical Genetics, Erasmus University Medical Center, 3015 Rotterdam, the Netherlands; ¹²Department of Medicine, Perelman School of Medicine, University of Pennsylvania, Philadelphia, PA 19104, USA; ¹³Department of Genetics, Perelman School of Medicine, University of Pennsylvania, Philadelphia, PA 19104, USA; ¹⁴Department of Molecular Genetics, Royal Devon and Exeter NHS Foundation Trust, Barrack Road, EX2 5DW Exeter, UK; ¹⁵Centro de Genética Médica Jacinto de Magalhães, Centro Hospitalar do Porto, CHP, E.P.E., 4099-028 Porto, Portugal; ¹⁶Unit for Multidisciplinary Research in Biomedicine, Abel Salazar Institute of Biomedical Sciences, University of Porto, 4099-028 Porto, Portugal; ¹⁷College of Medicine and Health, University of Exeter, Barrack Road, EX2 5DW Exeter, UK; ¹⁸Department of Neurology, Donders Institute for Brain, Cognition, and Behavior, Radboud University Medical Center, 6525 GA Nijmegen, the Netherlands; ¹⁹Department of Laboratory Medicine, Translational Metabolic Laboratory, Radboud University Medical Center, 6525 GA Nijmegen, the Netherlands; ²⁰Department of Pathology and Laboratory Medicine, Children's Hospital of Philadelphia, Philadelphia, PA 19104, USA; ²¹Department of Pathology and Laboratory Medicine, Perelman School of Medicine, University of Pennsylvania, Philadelphia, PA 19104, USA

²²These authors contributed equally

*Correspondence: hem@email.chop.edu (M.H.), arjan.debrouwer@radboudumc.nl (A.P.M.d.B.)

<https://doi.org/10.1016/j.ajhg.2021.05.010>

© 2021 American Society of Human Genetics.



ALG12-CDG (MIM: 607143), and DPAGT1-CDG (MIM: 608093). If this degradative process fails to effectively remove misfolded and abnormal proteins from the ER, then the unfolded protein response (UPR) is initiated.^{17–20} The UPR is critical to maintain cellular homeostasis. In mammals, three classical ER stress markers are known to reflect induction of the UPR: protein kinase RNA-like endoplasmic reticulum kinase (PERK), activating transcription factor 6 (ATF6), and inositol requiring enzyme 1 (IRE1).^{21,22} Upon protein overload in the ER, UPR signaling via the PERK, ATF6, and IRE1 pathways is activated to increase ER capacity, inhibit translation, and stimulate the removal of excess and misfolded proteins.^{23–26} Persistent activation of UPR can lead to apoptosis.^{27–29}

Here, we describe seven independent families with 11 individuals with bi-allelic protein-truncating variants and one additional individual with a compound heterozygous missense variant in *EDEM3* (MIM: 610214) identified by exome sequencing (Figure 1) and collected through GeneMatcher.³⁰ The parents or legal guardians provided written informed consent. All relevant approvals from the institutional review boards and ethics committees of the participating institutions were obtained. In affected individuals from families 1 and 2, a bi-allelic frameshift deletion, c.1859del (p.Ile620Thrfs*7), was identified in *EDEM3* (GenBank: NM_025191.3; Figure 1). Additionally, two frameshift variants, c.2001dup (p.Ala668Serfs*9) and c.1369del (p.Arg457Glufs*28), were identified in family 3. In family 4, a bi-allelic nonsense variant, c.940A>T (p.Arg314*), was found, resulting from maternal uniparental isodisomy of chromosome 1. In family 5, a canonical splice site donor variant, c.853+1G>T, and a nonsense variant, c.1407T>A (p.Tyr469*), were identified, and in family 6, a bi-allelic frameshift deletion, c.1382_1385del (p.Phe461Serfs*23) was identified. Finally, in family 7, the compound heterozygous changes c.182A>G (p.Asp61Gly) and c.1366G>A (p.Asp456Asn) were identified. Sanger sequencing showed that the affected individuals were either homozygous or compound heterozygous for the identified *EDEM3* variants. The unaffected parents were all heterozygous carriers. The p.Asp61Gly missense variant was found in six heterozygous individuals, out of 218,508 alleles, in gnomAD (rs777353823) and was predicted to be “disease causing” by MutationTaster³¹ but “tolerated” by SIFT.³² The p.Asp456Asn missense variant was not present in gnomAD and was predicted to be “disease causing” by both MutationTaster and SIFT. Both are present in the so-called “Glyco_Hydro_47 domain,” which is essential for the α -mannosidase activity of the protein.

Affected individuals from family 1 and 2 have the identical c.1859del (p.Ile620Thrfs*7) *EDEM3* variant, but there are no records of inter-familial consanguinity in these families. Comparison of the exome data from two affected individuals from family 1 and from one affected individual from family 2 indicated that these three individuals carried a common identical region of homozygosity of 3.16 Mb (chr1: 182,993,025–186,157,274, Hg19) surrounding

EDEM3. In addition, 96 healthy control individuals in the Romani population in Portugal were screened for the presence of this variant, among whom one heterozygous allele was detected. Because families 1 and 2 are of Portuguese Romani origin, this suggests a possible founder effect.

All affected individuals presented with developmental delay and/or intellectual disability (ID) and speech delay (Table S1). Hypotonia was present in six out of 12 persons. Dysmorphic facial features, such as narrow palpebral fissures (6/12), epicanthal folds (6/12), increased nasal height (8/12), bulbous nasal tip (6/12), hypoplastic alae nasi (9/12), short philtrum (6/12), thin upper lip (9/12), and retrognathia (6/12) were also found in half or more of the affected individuals. Additionally, gastroesophageal reflux was observed in three persons, and two individuals had early feeding difficulties requiring a nasogastric tube; of these, one individual needed a percutaneous endoscopic gastrostomy placement. Brain magnetic resonance imaging (MRI) of affected individuals from families 2, 3, and 5 did not detect structural abnormalities or myelination defects.

The protein-truncating variants identified in this study are expected to result in either reduced protein levels, due to degradation of mRNA via nonsense-mediated decay (NMD), or a truncated protein.^{33,34} Accordingly, quantitative real-time PCR analysis showed that *EDEM3* mRNA levels in Epstein-Barr virus-transformed lymphoblastoid cell lines (EBV-LCLs) from affected individuals in family 1 were significantly decreased to 17% as compared to healthy controls ($p = 0.0078$; Figure 2A) and could be rescued with cycloheximide (CHX), an inhibitor of NMD, suggesting that the bi-allelic c.1859del frameshift variant triggers NMD. We repeated these experiments in fibroblasts from affected individuals in families 1 and 3 and confirmed that *EDEM3* is degraded to 18% of normal levels by NMD ($p = 0.0015$; Figure 2B). Immunoblots of *EDEM3* were performed in two individual fibroblast cell lines from these two families. These demonstrated the absence of *EDEM3* in individual IV-4 (family 1) and individual II-1 (family 3) consistent with loss of function of *EDEM3* (Figure 3C). Because the function of *EDEM3* could theoretically be compensated by *EDEM1*,³⁵ we quantified *EDEM1* (MIM: 607673) RNA levels in affected and control fibroblast cell lines. *EDEM1* levels were at 97% of normal levels ($p = 0.9373$) in fibroblast cell lines from affected individuals (Figure 2C). The comparable levels of *EDEM1* in affected and control fibroblast cell lines seems to suggest that *EDEM1* expression does not compensate for the reduction of *EDEM3* in these cells.

Previous studies have shown that *EDEM3* belongs to a group of proteins that accelerate the degradation of misfolded glycoproteins in the ER. It is one of the ER 1,2- α mannosidases and specifically trims M8B to M7 (Figure 3A), which is then recognized by lectin OS-9 and targeted for degradation.^{8–11} We hypothesized that loss of M8B to M7 trimming activity would result in

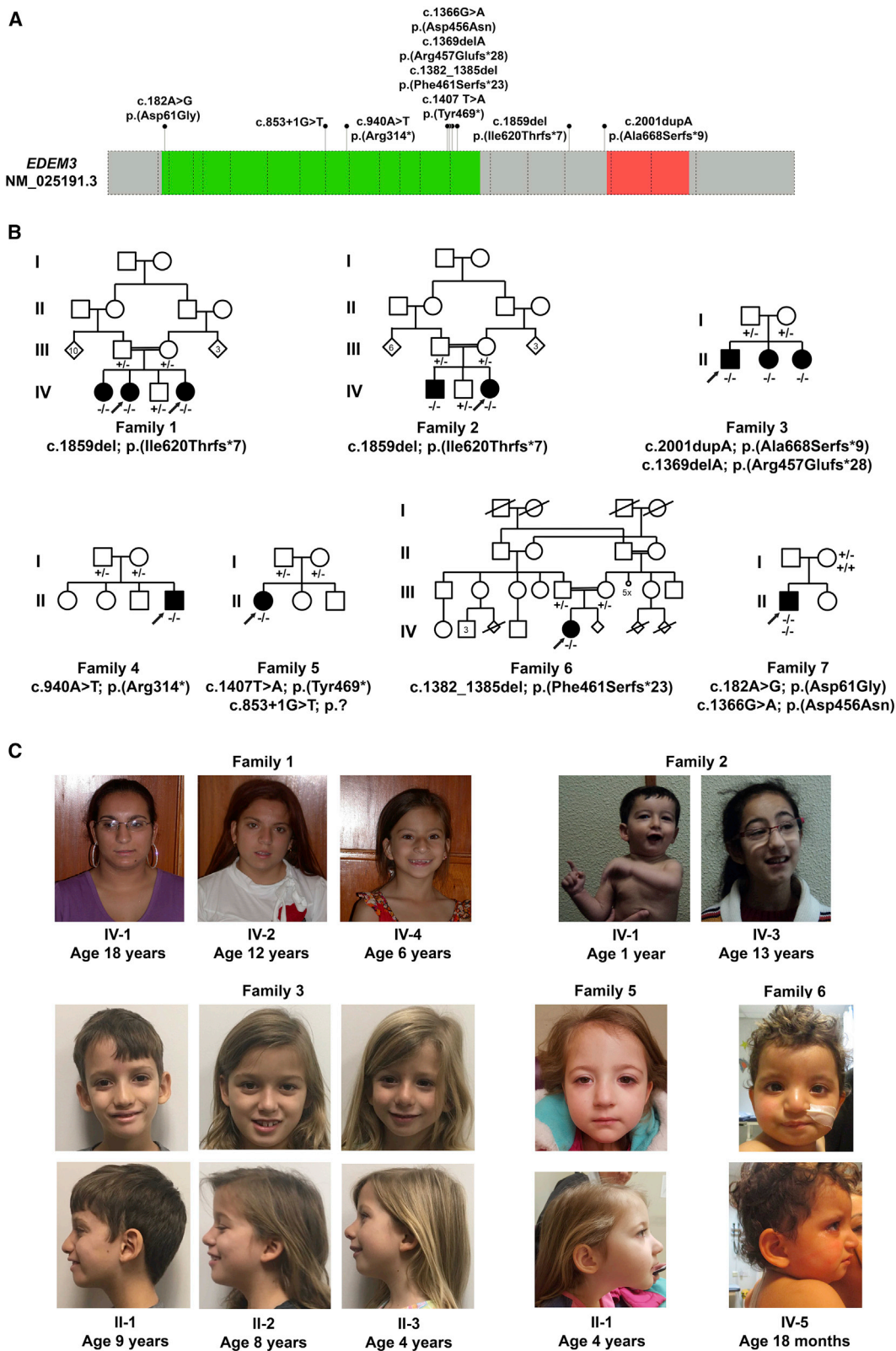


Figure 1. Bi-allelic variants in *EDEM3* lead to developmental delay or intellectual disabilities and dysmorphic features

(A) Schematic representation of human *EDEM3* including the positions and the predicted effect on protein level of the seven identified variants in this study. The green box represents the Glyco_Hydro_47 domain, and the red box represents the protease-associated (PA) domain. Dashed boxes represent exons.

(B) Pedigrees of *EDEM3*-CDG families including the presence of the mutation. –, mutation present; +, wild-type.

(C) Craniofacial features of affected individuals, including narrow palpebral fissures, epicanthal folds, increased nasal height, bulbous nasal tip, hypoplastic alae nasi, short philtrum, thin upper lip, and retrognathia.

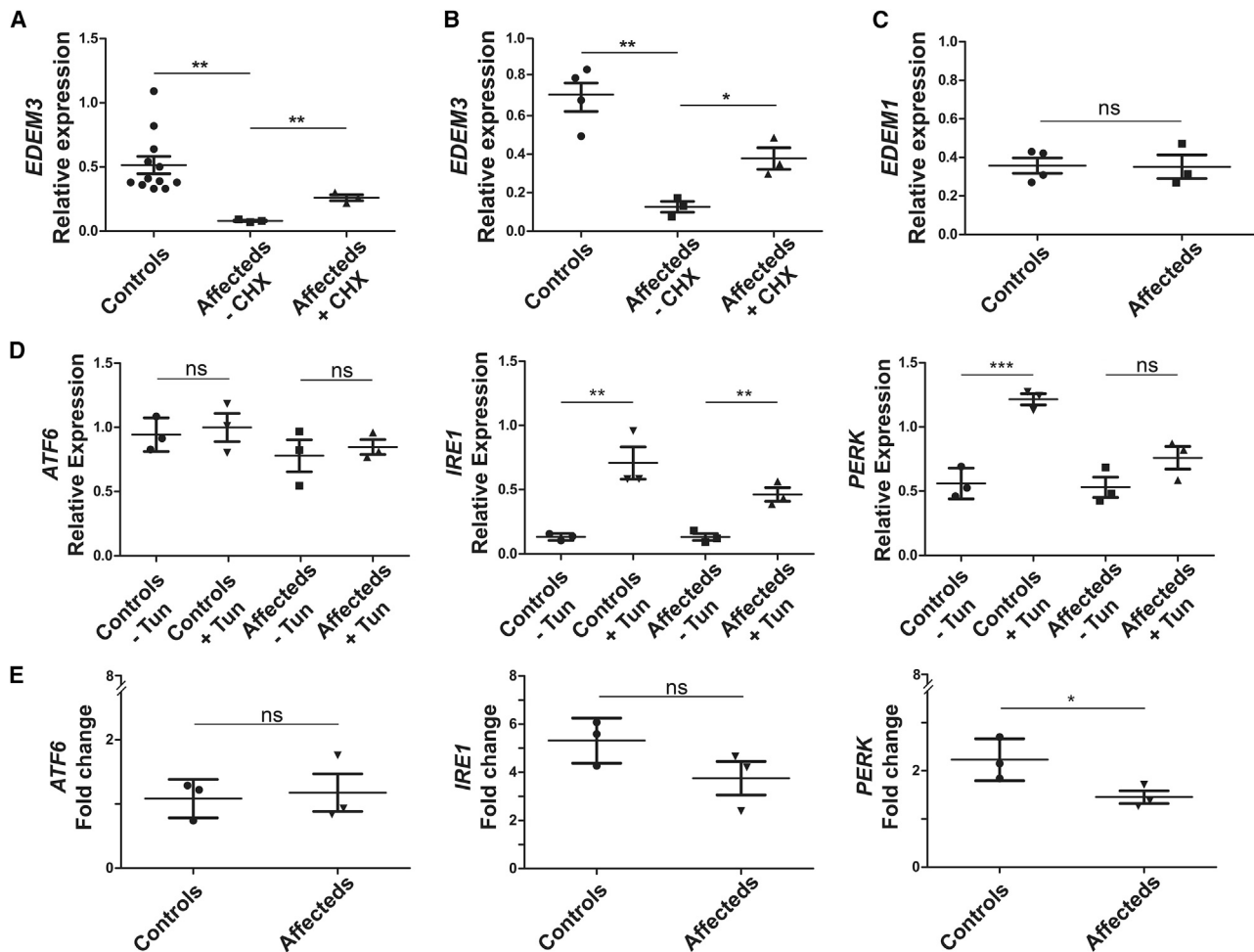


Figure 2. Relative expression of *EDEM3* mRNA and expression analysis of UPR markers

(A) A significant decrease of mRNA levels is seen between relative expressions of *EDEM3* in EBV-LCL from three affected individuals of family 1 with the bi-allelic c.1859del frameshift variant ($n = 3$) compared to healthy controls ($n = 12$; $p = 0.0078$) and samples treated with cycloheximide (CHX; $n = 3$; $p = 0.0016$), normalized according to three housekeeping genes.

(B) *EDEM3* expression in fibroblast cell lines from family 1 (individual IV-4) and family 3 (individuals II-1 and II-2) confirming these results ($p = 0.0015$ and $p = 0.0161$ for CHX). Four controls were used.

(C) *EDEM1* expression in fibroblast cell lines from family 1 (individual IV-4) and family 3 (individuals II-1 and II-2) showing normal expression levels ($p = 0.9373$). Four controls were used.

(D) Analysis of total mRNA from EBV-LCL cell lines from controls revealed increased mRNA expression after treatment with tunicamycin (Tun) of *IRE1* and *EIF2AK3* (*PERK*) but not of *ATF6*.

(E) Affected individuals' mRNA from family 1 showed significantly decreased induction of *PERK* expression when compared to controls ($p = 0.020$), whereas *ATF6* and *IRE1* did not change significantly ($p = 0.423$ and $p = 0.091$, respectively). Experiments in (D) and (E) were performed with three control cell lines and three cell lines from affected individuals. Bars indicate mean values. Error bars represent standard deviation. ns, not significant; * $p < 0.05$; ** $p < 0.01$; *** $p < 0.001$.

accumulation of abnormal N-glycans. Therefore, we determined the N-glycan profiles of total cellular glycoproteins prepared from a fibroblast cell line of a control individual and of an affected individual. Total N-glycan analysis via mass spectrometry in the affected individual's fibroblast cell line showed accumulation of M9 and M8 and reduced M7 and $\text{Man}_6\text{GlcNAc}_2$ (M6) levels (Figure S1). To study more precisely the impact of *EDEM3* deficiency, we also analyzed the N-glycan profile after a pulse-chase experiment by using $[2\text{-}^3\text{H}]\text{mannose}$ as precursor. We tested whether the variants in *EDEM3* affect the level of glycoproteins in fibroblast cell lines of individuals from families 1 and 3. In control fibroblast cells, we observed the anti-

patented levels of M8, M9, and $\text{Glc}_1\text{Man}_9\text{GlcNAc}_2$ (G1M9; Figure 3B). *EDEM3* deficient cells from members of family 1 and 3 exhibited a similar pattern of N-glycan structures, although with increased accumulation of M5 and G1M5. The structure of these two species was confirmed with either saitoi or jack bean α -mannosidase treatment, as the G1M5 terminal glucose conferred substantial protection of the peak from the mannosidases (Figure S3). After 2 h of chase, the peaks for M7 and M4 did not appear in the cells of affected individuals (Figure 3B), indicating that the 1,2- α mannose residues were not removed from the M8B and M5 N-glycans during the chase, which is consistent with the absence of the biological function of

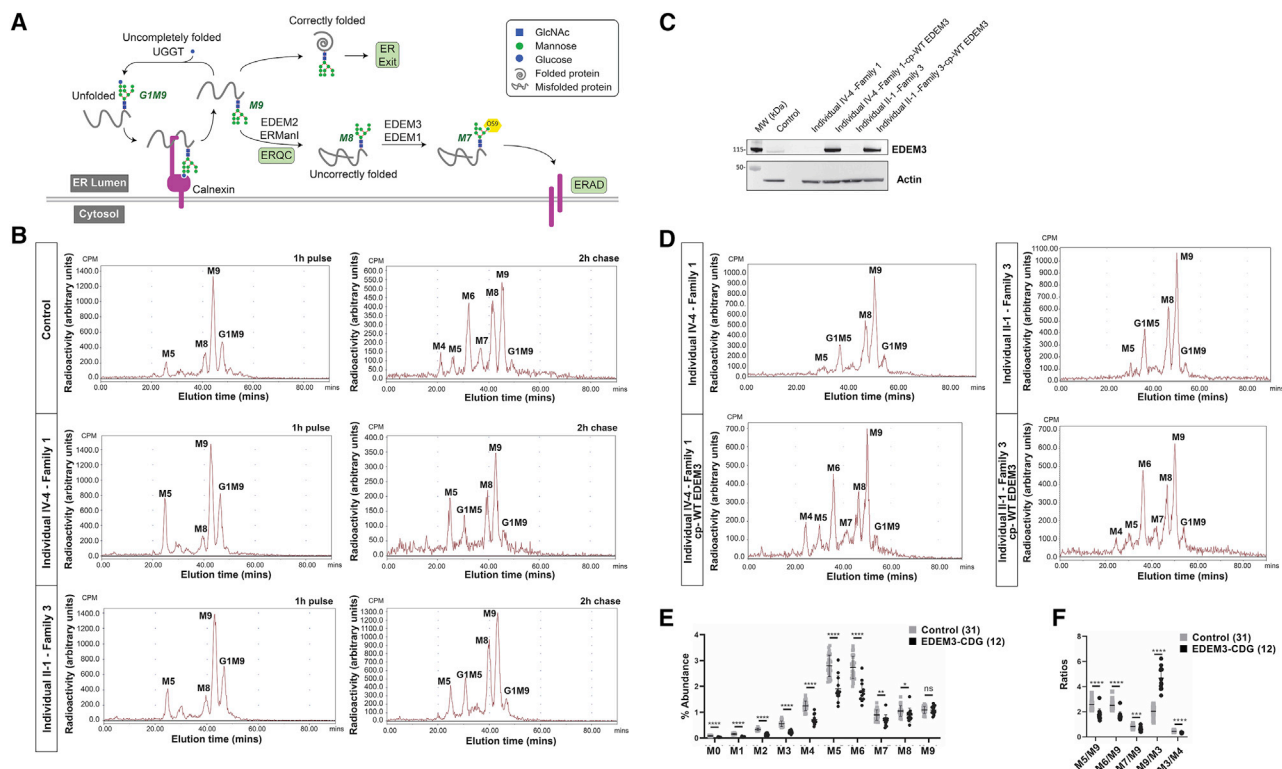


Figure 3. N-glycosylation pathway and N-glycan analysis of fibroblasts and plasma of human subjects

(A) N-glycosylation pathway and the role of EDEM proteins in the mannose trimming and targeting for protein degradation in the cytosol.

(B) Accumulation of G1M5 and M5 and a lack of M7, M6, and M4 on newly synthesized N-glycoproteins in two EDEM3-CDG fibroblast cell lines from affected individuals. Fibroblasts from family 1 (individual IV-4) and family 3 (individual II-1) and one control individual were incubated with [2-³H]mannose for 1 h and chased during 2 h.

(C) Immunoblot analysis of fibroblasts from individual IV-4 (family 1) and individual II-1 (family 3) before and after complementation with wild-type (WT) EDEM3. Total cell lysates were prepared and subjected to SDS-PAGE and immunoblot analysis with indicated antibodies.

(D) N-glycan analysis of fibroblasts from individual IV-4 and individual II-1 complemented with WT EDEM3 after incubation with [2-³H]mannose for 1 h and chasing for 2 h.

(E) Percent abundance of plasma N-glycan species obtained from EDEM3-CDG-affected individuals and control individuals.

(F) Plot of ratio of plasma N-glycan species. Bars indicate mean values. Error bars represent standard deviation. Indicated p values from Student's t test, ns, not significant; *p < 0.05; **p < 0.01; ***p < 0.001; ****p < 0.0001.

EDEM3 (Figure 3A). We speculate that the M5 corresponds to the biosynthetic oligosaccharide precursor synthesized as a lipid-linked oligosaccharide and not generated through mannose trimming. The lipid-linked oligosaccharides profiles did not show M5 accumulation (data not shown). All together, these results may indicate that EDEM3 deficiency impairs lipid-linked oligosaccharide synthesis and that the M5 is transferred onto newly synthesized proteins and glucosylated to form G1M5 by the UDP-Glc:glycoprotein glucosyltransferase during calnexin cycle (Figure 3A).³⁶

To evaluate the N-glycosylation of secreted glycoproteins, we studied the N-glycan profile of total plasma glycoproteins from all affected individuals, including the individual with compound heterozygous missense variants, by using our recently described and clinically validated semiquantitative N-glycan assay.³⁷ The N-glycan profiles from affected individuals showed decreased levels of low mannose N-glycan species M3–M7 (Figure 3C) with pre-

served normal M8 and M9 or sometimes mildly increased abundance of M9 as compared to control subjects. Ratios of the N-glycan abundances were also explored, and affected individuals had prominently decreased ratios of M5:M9, M6:M9, and M7:M9 as well as decreased M3:M4 (Figure 3D; Table S2). M6:M9 ratio provided the highest discrimination between tested obligate heterozygotes (parents, n = 4) and affected individuals (n = 12; Table S3). In theory, M3 can be produced by multiple pathways with or without EDEM3; thus, we used M9:M3 ratio to normalize M9 abundance. M9:M3 was increased in all 12 affected individuals. Stepwise ratio analysis for plasma N-linked polymannose species showed a reduction of M7:M8 that is significant in affected individuals, consistent with EDEM3's being the key enzyme in trimming M8B to M7 on secreted glycoproteins (Table S3).^{9,10} Interestingly, M3:M4 ratio was also reduced in all 12 affected individuals tested, consistent with a possible role of EDEM3 in trimming M5 to shorter polymannose glycans, as suggested by the pulse

chase data. EDEM3's involvement in trimming of both M8 and M5 emphasizes that it is an essential ER mannosidase in humans. Of note, human transferrin was normally glycosylated in the common clinical screening test for CDG in the three affected individuals from family 3.

N-glycan profiles were also obtained from *Edem3* knockout (KO) mice (Figure S4). Although *Edem3* KO mice did not present with any obvious phenotype, subtle changes have been noted, such as reduced weight of brains and body and largely skewed ratios of homozygous KO pups versus heterozygous and wild-type pups. The profiles were acquired via a previously described method.³⁷ Similar to affected individuals, plasma from mice showed decreased ratios of M5:M9, M6:M9, and M7:M9 ($p < 0.02$; Figure S5B). In addition, mouse plasma proteins had significantly increased abundance of M8 and M9 ($p < 0.01$; Figure S5A). We also assayed mouse brain lysate for N-glycan profiles (Figure S5C) and ratios (Figure S5D). While plasma N-glycans reflect glycosylation of mature secreted glycoproteins and glycopeptides, N-glycan profiling of mouse tissue also includes cellular glycoproteins. Similar to mouse plasma N-glycan profiling, mouse brain showed increased high-mannose M8 and M9 N-glycan species (Figure S5C) and decreased ratios of M5:M9 and M6:M9 (Figure S5D).

N-glycan analysis of both *Edem3* KO mouse brain and plasma showed significant increases of the abundance M8 and M9. Thus, the known function of EDEM3 in trimming M8B is most likely shared by both humans and mice. In humans, not all the EDEM3-deficient individuals have increased M8 or M9 in the plasma. Instead, M9:M3 ratio is increased in all 12 affected individuals, providing a more sensitive diagnostic biomarker than M8 or M9 abundance in plasma. N-linked M3 and M4 are newly discovered small high-mannose species with low abundance on normal plasma glycoproteins.³⁷ Increases of M3 and M4 abundances have been reported as important diagnostic biomarkers for type I CDG subtypes, including PMM2-CDG, MPI-CDG, ALG3-CDG, and ALG9-CDG.^{37–39} Significantly reduced abundance of N-linked M3 with a decreased M3:M4 ratio ($p < 0.0001$), however, has not been reported before. The reduction of M3 in all of the affected individuals suggests that a large portion of N-linked M3 in the control population is probably derived from glycan trimming ultimately involving human EDEM3 (Figure 3A). In the plasma from *Edem3* KO mice, M3:M4 ratio is not decreased (Figures S5B and S5D). Instead of increased M7:M8 ratio in humans, the increased M6:M7 ratio is the most significant, which may reflect a difference in overall substrate specificity between human and mouse EDEM3. The glycosylation abnormalities in both cellular or tissue proteins and secreted mature proteins indicate a global impact on protein N-glycosylation in EDEM3 deficiency. Consistent with our findings, it was previously demonstrated that EDEM3 participates in mannose trimming from total glycoproteins and not just misfolded proteins for ERAD.¹⁰ Therefore, we propose this deficiency to be EDEM3-CDG.

The finding of abnormal N-glycan profiling pattern with reduced M3:M4, M5:M9, M6:M9, and M7:M9 ratios and increased M9:M3 among EDEM3-CDG-affected individuals provides additional diagnostic biomarkers for validating variants of uncertain significance, i.e., missense variants in *EDEM3*. One of the 12 EDEM3-CDG-affected individuals showed normal plasma of M5:M9 and M6:M9 ratios but also showed the lowest plasma N-linked M3:M4 ratio at 0.27 (normal 0.39–0.56) and a significantly increased M9:M3 ratio at 3.30 (normal 1.16–2.92) in this cohort. Therefore, the combination of high M9:M3 and low M3:M4 ratios might also provide diagnostic clues for EDEM3-CDG when M5:M9 and M6:M9 ratios are normal.

G1M5 accumulation is a marker for an impaired UPR.³⁶ Given the role of EDEM3 in gpERAD and its association with the UPR, we tested whether the UPR, a key quality-control process in the cell that is activated in response to the accumulation of misfolded proteins,²² is affected in EDEM3-CDG. Quantitative real-time PCR analysis of total mRNA from EBV-LCLs from affected individuals showed decreased stimulation of *ERN1* (*IRE1* [MIM: 604033]) and *EIF2AK3* (*PERK* [MIM: 604032]) when cells were treated with tunicamycin, a UPR-inducing compound, as compared to controls (Figure 2D). *ATF6* (MIM: 605537) expression levels were similar. The difference in *IRE1* expression levels was not significant ($p = 0.091$), whereas the decreased stimulation of *PERK* expression levels in cell lines from affected individuals was significant ($p = 0.020$; Figure 2E), suggesting that the UPR is impaired in EDEM3-CDG or that these cell lines have an increased capacity to eliminate misfolded proteins.

EDEM3 was recently implicated in triglyceride metabolism. A low-frequency EDEM3 missense variant in the protease-associated domain (rs78444298, p.Pro746Ser, minor allele frequency ~1.5%) was associated with an approximately 5% decrease in triglyceride levels.⁴⁰ In our subjects for whom fasting triglyceride levels are available (Table S1), all triglyceride measurements were within the normal range. This most likely reflects the multiple metabolic pathways influencing triglyceride levels and makes the use of triglycerides as a diagnostic marker for EDEM3-CDG challenging.

In conclusion, we show that bi-allelic *EDEM3* variants cause EDEM3-CDG, a CDG with non-specific developmental delay and/or intellectual disability. Several affected individuals also have mild facial dysmorphisms. Given the increased accessibility of blood for clinical testing, semiquantitative N-glycan analysis provides additional diagnostic biomarkers for validating variants of uncertain significance that may be identified on molecular genetic testing. Further functional studies are necessary to determine the precise pathophysiological mechanism of EDEM3-CDG.

Data and code availability

All data that are relevant to this research are presented in this paper.

Supplemental information

Supplemental information can be found online at <https://doi.org/10.1016/j.ajhg.2021.05.010>.

Acknowledgments

We are grateful to the families that have participated to this study. This work was supported by the EU FP7 large-scale integrating project Genetic and Epigenetic Networks in Cognitive Dysfunction (241995) (to H.v.B.); National Institutes of Health (NIH) grants 5R01GM115730-03 (to M.H.), U54 NS115198 (to A.C.E. and M.H.), and T32GM008638 (to A.C.E.); and the Transatlantic Network of Excellence grant (10CVD03) from the Fondation Leducq and NIH NHGRI U01HG006398 (to D.J.R.). Family 4 was enrolled in the CAUSES Study; investigators include Shelin Adam, Christele Du Souich, Alison Elliott, Anna Lehman, Jill Mwenifumbo, Tanya Nelson, Clara Van Karnebeek, and Jan Friedman; it is funded by Mining for Miracles, British Columbia Children's Hospital Foundation (grant number F15-01355) and Genome British Columbia (grant number F16-02276). D.L.P. is recipient of a CAPES Fellowship (99999.013311/2013-01). X.B. is supported by an AHA career development award (19CDA34630032).

Declaration of interests

The authors declare no competing interests.

Consortia

The members of the CAUSES Study are Shelin Adam, Christele Du Souich, Alison Elliott, Anna Lehman, Jill Mwenifumbo, Tanya Nelson, Clara Van Karnebeek, and Jan Friedman.

Received: April 14, 2020

Accepted: May 19, 2021

Published: June 17, 2021

Web resources

gnomAD, <https://gnomad.broadinstitute.org>

OMIM, <https://www.omim.org/>

References

1. Brodsky, J.L. (2012). Cleaning up: ER-associated degradation to the rescue. *Cell* 151, 1163–1167.
2. Needham, P.G., and Brodsky, J.L. (2013). How early studies on secreted and membrane protein quality control gave rise to the ER associated degradation (ERAD) pathway: the early history of ERAD. *Biochim. Biophys. Acta* 1833, 2447–2457.
3. Smith, M.H., Ploegh, H.L., and Weissman, J.S. (2011). Road to ruin: targeting proteins for degradation in the endoplasmic reticulum. *Science* 334, 1086–1090.
4. Thibault, G., and Ng, D.T.W. (2012). The endoplasmic reticulum-associated degradation pathways of budding yeast. *Cold Spring Harb. Perspect. Biol.* 4, a013193.
5. Aebi, M., Bernasconi, R., Clerc, S., and Molinari, M. (2010). N-glycan structures: recognition and processing in the ER. *Trends Biochem. Sci.* 35, 74–82.
6. Molinari, M. (2007). N-glycan structure dictates extension of protein folding or onset of disposal. *Nat. Chem. Biol.* 3, 313–320.
7. Hosokawa, N., Tremblay, L.O., You, Z., Herscovics, A., Wada, I., and Nagata, K. (2003). Enhancement of endoplasmic reticulum (ER) degradation of misfolded Null Hong Kong alpha1-antitrypsin by human ER mannosidase I. *J. Biol. Chem.* 278, 26287–26294.
8. Mast, S.W., Diekman, K., Karaveg, K., Davis, A., Sifers, R.N., and Moremen, K.W. (2005). Human EDEM2, a novel homolog of family 47 glycosidases, is involved in ER-associated degradation of glycoproteins. *Glycobiology* 15, 421–436.
9. Ninagawa, S., Okada, T., Sumitomo, Y., Kamiya, Y., Kato, K., Horimoto, S., Ishikawa, T., Takeda, S., Sakuma, T., Yamamoto, T., and Mori, K. (2014). EDEM2 initiates mammalian glycoprotein ERAD by catalyzing the first mannose trimming step. *J. Cell Biol.* 206, 347–356.
10. Hirao, K., Natsuka, Y., Tamura, T., Wada, I., Morito, D., Natsuka, S., Romero, P., Sleno, B., Tremblay, L.O., Herscovics, A., et al. (2006). EDEM3, a soluble EDEM homolog, enhances glycoprotein endoplasmic reticulum-associated degradation and mannose trimming. *J. Biol. Chem.* 281, 9650–9658.
11. Hosokawa, N., Tremblay, L.O., Sleno, B., Kamiya, Y., Wada, I., Nagata, K., Kato, K., and Herscovics, A. (2010). EDEM1 accelerates the trimming of alpha1,2-linked mannose on the C branch of N-glycans. *Glycobiology* 20, 567–575.
12. Olivari, S., Cali, T., Salo, K.E.H., Paganetti, P., Ruddock, L.W., and Molinari, M. (2006). EDEM1 regulates ER-associated degradation by accelerating de-mannosylation of folding-defective polypeptides and by inhibiting their covalent aggregation. *Biochem. Biophys. Res. Commun.* 349, 1278–1284.
13. Hosokawa, N., Kamiya, Y., Kamiya, D., Kato, K., and Nagata, K. (2009). Human OS-9, a lectin required for glycoprotein endoplasmic reticulum-associated degradation, recognizes mannose-trimmed N-glycans. *J. Biol. Chem.* 284, 17061–17068.
14. Fujita, E., Kouroku, Y., Isoai, A., Kumagai, H., Misutani, A., Matsuda, C., Hayashi, Y.K., and Momoi, T. (2007). Two endoplasmic reticulum-associated degradation (ERAD) systems for the novel variant of the mutant dysferlin: ubiquitin/proteasome ERAD(I) and autophagy/lysosome ERAD(II). *Hum. Mol. Genet.* 16, 618–629.
15. Hirsch, C., Gauss, R., Horn, S.C., Neuber, O., and Sommer, T. (2009). The ubiquitylation machinery of the endoplasmic reticulum. *Nature* 458, 453–460.
16. Rashid, H.-O., Yadav, R.K., Kim, H.-R., and Chae, H.-J. (2015). ER stress: Autophagy induction, inhibition and selection. *Autophagy* 11, 1956–1977.
17. Guerriero, C.J., and Brodsky, J.L. (2012). The delicate balance between secreted protein folding and endoplasmic reticulum-associated degradation in human physiology. *Physiol. Rev.* 92, 537–576.
18. Shang, J., Körner, C., Freeze, H., and Lehrman, M.A. (2002). Extension of lipid-linked oligosaccharides is a high-priority aspect of the unfolded protein response: endoplasmic reticulum stress in Type I congenital disorder of glycosylation fibroblasts. *Glycobiology* 12, 307–317.
19. Lecca, M.R., Wagner, U., Patrignani, A., Berger, E.G., and Henret, T. (2005). Genome-wide analysis of the unfolded protein response in fibroblasts from congenital disorders of glycosylation type-I patients. *FASEB J.* 19, 240–242.
20. Yuste-Checa, P., Vega, A.I., Martín-Higueras, C., Medrano, C., Gámez, A., Desviat, L.R., Ugarte, M., Pérez-Cerdá, C., and Pérez, B. (2017). DPAGT1-CDG: Functional analysis of disease-causing pathogenic mutations and role of endoplasmic reticulum stress. *PLoS ONE* 12, e0179456.

21. Walter, P., and Ron, D. (2011). The unfolded protein response: from stress pathway to homeostatic regulation. *Science* 334, 1081–1086.
22. Ron, D., and Walter, P. (2007). Signal integration in the endoplasmic reticulum unfolded protein response. *Nat. Rev. Mol. Cell Biol.* 8, 519–529.
23. Kim, I., Xu, W., and Reed, J.C. (2008). Cell death and endoplasmic reticulum stress: disease relevance and therapeutic opportunities. *Nat. Rev. Drug Discov.* 7, 1013–1030.
24. Kimata, Y., and Kohno, K. (2011). Endoplasmic reticulum stress-sensing mechanisms in yeast and mammalian cells. *Curr. Opin. Cell Biol.* 23, 135–142.
25. Termine, D.J., Moremen, K.W., and Sifers, R.N. (2009). The mammalian UPR boosts glycoprotein ERAD by suppressing the proteolytic downregulation of ER mannosidase I. *J. Cell Sci.* 122, 976–984.
26. Xiang, C., Wang, Y., Zhang, H., and Han, F. (2017). The role of endoplasmic reticulum stress in neurodegenerative disease. *Apoptosis* 22, 1–26.
27. Fribley, A., Zhang, K., and Kaufman, R.J. (2009). Regulation of apoptosis by the unfolded protein response. *Methods Mol. Biol.* 559, 191–204.
28. Sano, R., and Reed, J.C. (2013). ER stress-induced cell death mechanisms. *Biochim. Biophys. Acta* 1833, 3460–3470.
29. Tabas, I., and Ron, D. (2011). Integrating the mechanisms of apoptosis induced by endoplasmic reticulum stress. *Nat. Cell Biol.* 13, 184–190.
30. Sobreira, N., Schietecatte, F., Valle, D., and Hamosh, A. (2015). GeneMatcher: a matching tool for connecting investigators with an interest in the same gene. *Hum. Mutat.* 36, 928–930.
31. Schwarz, J.M., Cooper, D.N., Schuelke, M., and Seelow, D. (2014). MutationTaster2: mutation prediction for the deep-sequencing age. *Nat. Methods* 11, 361–362.
32. Sim, N.-L., Kumar, P., Hu, J., Henikoff, S., Schneider, G., and Ng, P.C. (2012). SIFT web server: predicting effects of amino acid substitutions on proteins. *Nucleic Acids Res.* 40, W452–7.
33. Maquat, L.E. (1995). When cells stop making sense: effects of nonsense codons on RNA metabolism in vertebrate cells. *RNA* 1, 453–465.
34. Baker, K.E., and Parker, R. (2004). Nonsense-mediated mRNA decay: terminating erroneous gene expression. *Curr. Opin. Cell Biol.* 16, 293–299.
35. Shenkman, M., Ron, E., Yehuda, R., Benyair, R., Khalaila, I., and Lederkremer, G.Z. (2018). Mannosidase activity of EDEM1 and EDEM2 depends on an unfolded state of their glycoprotein substrates. *Commun. Biol.* 1, 172.
36. Foulquier, F., Duvet, S., Klein, A., Mir, A.-M., Chirat, F., and Cacan, R. (2004). Endoplasmic reticulum-associated degradation of glycoproteins bearing Man5GlcNAc2 and Man9GlcNAc2 species in the MI8-5 CHO cell line. *Eur. J. Biochem.* 271, 398–404.
37. Chen, J., Li, X., Edmondson, A., Meyers, G.D., Izumi, K., Ackermann, A.M., Morava, E., Ficicioglu, C., Bennett, M.J., and He, M. (2019). Increased Clinical Sensitivity and Specificity of Plasma Protein N-Glycan Profiling for Diagnosing Congenital Disorders of Glycosylation by Use of Flow Injection-Electrospray Ionization-Quadrupole Time-of-Flight Mass Spectrometry. *Clin. Chem.* 65, 653–663.
38. Zhang, W., James, P.M., Ng, B.G., Li, X., Xia, B., Rong, J., Asif, G., Raymond, K., Jones, M.A., Hegde, M., et al. (2016). A Novel N-Tetrasaccharide in Patients with Congenital Disorders of Glycosylation, Including Asparagine-Linked Glycosylation Protein 1, Phosphomannomutase 2, and Mannose Phosphate Isomerase Deficiencies. *Clin. Chem.* 62, 208–217.
39. Davis, K., Webster, D., Smith, C., Jackson, S., Sinasac, D., Seargeant, L., Wei, X.-C., Ferreira, P., Midgley, J., Foster, Y., et al. (2017). ALG9-CDG: New clinical case and review of the literature. *Mol. Genet. Metab. Rep.* 13, 55–63.
40. Xu, Y.-X., Peloso, G.M., Nagai, T.H., Mizoguchi, T., Deik, A., Bullock, K., Lin, H., Musunuru, K., Yang, Q., Vasan, R.S., et al. (2020). EDEM3 Modulates Plasma Triglyceride Level through Its Regulation of LRP1 Expression. *iScience* 23, 100973.